RSC Advances

PAPER

View Article Online
View Journal | View Issue

Cite this: *RSC Adv.*, 2026, **16**, 30520

Copper-mediated stepwise polymerization of benzynes: construction of amphiphilic block copolymers and their self-assembly in water

Masahiro Sonobe,[a] Yu Kitazawa,[b] Masanobu Uchiyama[bc] and Mutsumi Kimura*[ab]

A novel synthetic approach for preparing well-defined amphiphilic poly(*ortho*-phenylene) (Po**P**) block copolymers *via* direct polymerization of benzynes has been reported. The polymerization of benzynes generated from *o*-trimethylsilyl aryl triflates with single hexyl or oligoethylene oxide side chains proceeded smoothly in the presence of copper(I) cyanide at room temperature, yielding Po**P** homopolymers with narrow molecular weight distributions. Block copolymers were prepared by the stepwise polymerization of two different benzynes, where the second benzyne was polymerized at the end of the Po**P** derived from the first benzyne. Spherical assemblies with diameters of 80–100 nm were formed from an amphiphilic block copolymer with a linear arrangement of hydrophobic and hydrophilic blocks in water. This synthetic approach opens new possibilities for various applications by enabling the design of well-defined Po**P**-based block copolymers.

Received 5th March 2026
Accepted 25th May 2026

DOI: 10.1039/d6ra01918h

rsc.li/rsc-advances

Introduction

Well-defined polyphenylene (PPs)-based architectures have been meticulously constructed by designing direct linkages among benzene rings.[1] The simple macromolecular structures for P**P**s are three linear architectures (P*p***P**, P*m***P**, and Po**P**) derived from the connections of disubstituted arene at the *para*, *meta*, and *ortho* positions (Scheme 1). Although P*p***P**s are rod-like molecules featuring through-bond conjugation, P*m***P**s and Po**P**s exhibit more complex conformational behavior. *Ortho*-Phenylene oligomers have been instrumental in our understanding of the folding phenomena leading to the formation of helices.[2–7] Since the first report by Simpkins,[8] a systematic series of discrete *ortho*-phenylene oligomers up to 48 mers have been synthesized using intricate stepwise aryl–aryl coupling methods such as Buchwald's active Suzuki–Miyaura coupling[9] and Asao–Yamamoto benzannulation[10] of *ortho*(phenylene-ethynylene) oligomers.

In contrast, highly reactive benzynes are polymerized to form polymeric Po**P**s by successive additions to their carbon–carbon triple bonds. In 2005, Ihara *et al.* reported the formation of an alternating copolymer of *o*-phenylene and 2,3-dihydroxypyridine units in the main chains *via* the reaction between benzyne and pyridine.[11] This is the first example of the polymerization of highly reactive benzyne species. To avoid the difficulty in controlling the reactivity of benzynes, Nozaki *et al.* reported a two-step synthetic approach for Po**P**s *via* the palladium-catalyzed coordination-insertion polymerization of a synthetic equivalent of benzyne and subsequent acid-promoted dehydration.[12] Finally, in 2015, Uchiyama *et al.* obtained Po**P** homopolymers by direct benzyne polymerization in the presence of monovalent copper reagents.[13] According to the computational analysis of the polymerization mechanism, the benzyne polymerization proceeded with the growth of polymer chains by forming an intermediate triangular complex of copper and benzyne after the initiation of copper(I) salts. The copper atom could move to one end of the chain during benzyne polymerization, and the successive insertion of the next benzyne into the terminal copper resulted in smooth chain growth depending on the feed molar ratio of benzyne and the monovalent copper initiator. Based on this mechanism, we considered that the diblock Po**P** copolymers, which consisted of a linear arrangement of two Po**P** blocks, could be derived from the stepwise polymerization of two *o*-trimethylsilyl aryl triflates

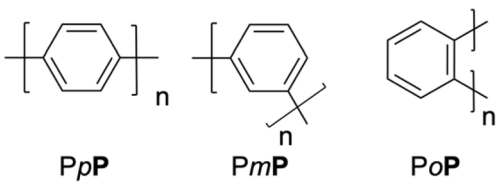

Scheme 1 Polyphenylenes.

[a]*Department of Chemistry and Materials, Faculty of Textile Science and Technology, Shinshu University, Ueda 386-8567, Japan. E-mail: mkimura@shinshu-u.ac.jp*
[b]*Research Initiative for Supra-Materials (RISM), Interdisciplinary Center for Cutting Edge Research (ICCER), Shinshu University, Japan*
[c]*Advanced Elements Chemistry Laboratory, Graduate School of Pharmaceutical Science, The University of Tokyo, 7-3-1 Hongo, Bunkyo-ku, Tokyo 113-0033, Japan*

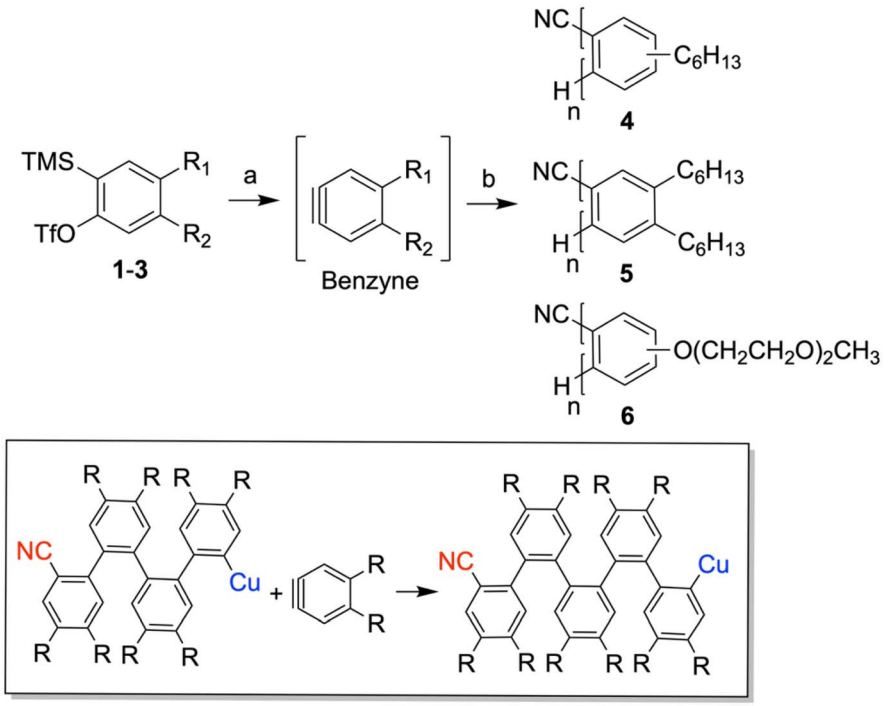

Fig. 1 Molecular structures of three monomers 1–3 for the polymerization of P*o*Ps.

substituted with different side chains. However, there have been no reports of P*o***P**-based block copolymers. The blocks in well-defined block copolymers exhibit thermodynamic incompatibility, resulting in microphase segregation and unique properties in solution and in the solid state.[14] This study focuses on the creation of nanostructures by self-assembly of amphiphilic diblock P*o***P** copolymers consisting of two blocks with hydrophobic and hydrophilic side chains in solution.

Results and discussion

Fig. 1 illustrates three *o*-trimethylsilyl aryl triflates, **1**, **2**, and **3**, designed as monomers of the hydrophobic and hydrophilic segments in diblock P*o***P** copolymers.[15–18] Monomer **1**, substituted with a single hexyl unit, was synthesized from 2-bromo-4-hexylphenol. First, the hydroxy unit of 2-bromo-4-hexylphenol was treated with hexamethyldisilazane (HMDS) for trimethylsilyl (TMS) esterification (Scheme S1). This was followed by the rearrangement of TMS by *n*-butyllithium and quenching with trifluoromethane sulfonic anhydride (Tf_2O). The other monomer, **2**, was prepared from 3,4-dichlorophenol in six synthetic steps, including the nickel-catalyzed Kumada–Tamao–Corriu coupling reaction.[19,20] Homopolymers **4** and **5** were prepared *via* direct benzyne polymerization in the presence of copper(I) cyanide (CuCN) in THF at room temperature (Scheme 2). This was performed after the *in situ* generation of benzyne from **1** or **2** with cesium fluoride (CsF) and 18-crown-6.[13] The feed molar ratio of the monomer and initiator ([**1**, **2**]/[CuCN]) was adjusted to 20 for all polymerizations. After 48 h, the reaction was quenched with an aqueous solution of NH_4Cl and the crude product was purified using gel permeation chromatography to remove low-molecular-weight compounds.

The degrees of polymerization of **4** and **5** were analyzed by gel-permeation chromatography (GPC) and matrix-assisted laser desorption ionization time-of-flight mass (MALDI-TOF-Ms) spectroscopy (Table 1 and Fig. 2). The number-average molecular weight (M_n) of **4** derived from **1** was estimated to be 7400 g mol^{-1} by GPC analysis based on poly(styrene) standards. This value is higher than the theoretical value calculated from the feed ratio ([**1**]/[CuCN] = 20), which we attribute to the larger hydrodynamic volume of the P*o***P** chain compared to the polystyrene standards, caused by the rigid backbone and the hexyl side chains.[12,13] The MALDI-TOF MS spectrum, providing absolute molecular weights, showed peaks in the range corresponding to the expected degree of polymerization. The MALDI-TOF-MS spectrum of **4** showed a series of peaks in the *m*/*z* range

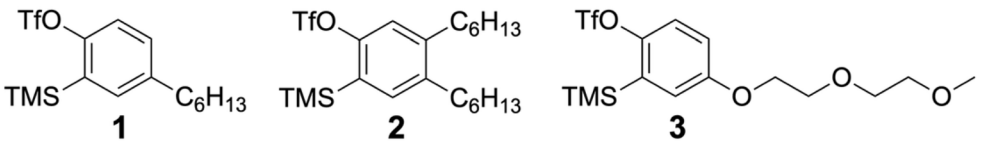

Scheme 2 Polymerization of benzynes generated from **1** and **2** in the presence of CuCN[a] and a plausible chain growth from tetramer to pentamer. [a] Reagents and conditions: (a) CsF, 18-crown-6, THF, rt; (b) CuCN and NH_4Cl aq.

Table 1 Homopolymerization of *o*-trimethylsilyl aryl triflates **1**, **2**, and **3** with CuCN in THF

Polymers	[Monomer]/[CuCN]	M_n [a]	M_w/M_n [a]	*m/z* gap [b]
4	3.3	1200	1.36	—
	10	3200	1.26	—
	20	7400	1.39	160.1
	50	14 000	1.33	—
5	20	3900	1.69	244.4
6	20	4300	1.44	194.1

[a] M_n and M_w/M_n were determined by GPC calibration using standard poly(styrene)s in THF. [b] *m/z* gaps were determined using MALDI-TOF-Ms spectra.

of 1000–8000, separated by a constant gap of 160.1 g mol^{-1} as shown in the inset of Fig. 2. This gap between the individual peaks was consistent with the molecular weight of the repeating unit ($C_{12}H_{16}$). The observed peak at *m/z* 2267.3 ([M + H]) was consistent with the calculated molecular weight of the 14 mer (*m/z* 160.13 × 14 (number of repeating units) + 1.0 (H) + 26.0 (CN) = 2266.8), supporting the introduction of the cyano group from the CuCN initiator on the terminal side of each polymer chain.[13]

Fig. 3a shows the GPC profiles for the polymerization of **1** by varying the feed molar ratio of **1** to CuCN. With an increase in [**1**]/[CuCN] ([**1**]/[CuCN] = 3.3, 10, 20, 50), the M_n value of **4** increased linearly from 1200 to 14 000 g mol^{-1} while maintaining an almost constant M_w/M_n value of approximately 1.3 (Fig. 3b). Thus, the degree of polymerization of benzyne depends on the concentration ratio of monomer **1** to the initially introduced CuCN initiator, and the number of polymer chains can be determined by the number of initiators. Moreover, the narrow molecular weight distribution (M_w/M_n) of benzyne polymerization initiated with CuCN suggests controlled growth of the polymer chain by continuously inserting benzyne into the active Cu located at one end of the polymer chain (Fig. 3c). ^{1}H NMR spectra of **4** in $CDCl_3$ exhibited aromatic proton signals at 4.4–7.4 ppm and hexyl group proton signals at 0.6–2.7 ppm (Fig. 4). Although the signal positions agree with those of the reported ^{1}H NMR spectra for *ortho*-phenylene oligomers and polymers, the spectrum for the aromatic proton signals of **4** is broadened and ill-defined.[4,7,21] Owing to the ring current effect, the aromatic protons at 6.0–7.5 ppm were upfield-shifted when the chain length of **4** was extended from 1200 to 14 000 g mol^{-1}. The observed ^{1}H NMR spectral features suggest that **4** contains different conformations formed by stacks of internal phenylene units in *ortho*-linkages. The other P*o*P, **5**, prepared by the polymerization of **2** substituted with two hexyl units at the same molar ratio of **2** and CuCN ([**2**]/[CuCN] = 20), exhibited a significantly lower M_n value than that of **4** (Table 1), and the ^{1}H NMR spectrum of **5** in $CDCl_3$ did not reveal an upfield shift of the aromatic proton signals (Fig. S1). This suggests the difficulty of chain growth in **5**,

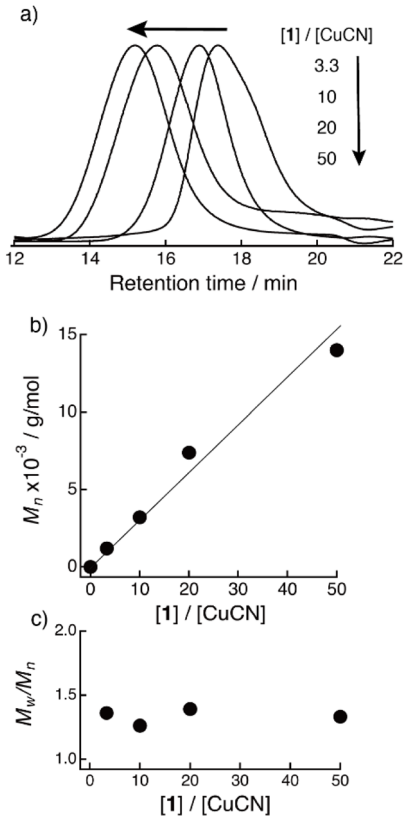

Fig. 3 (a) GPC profiles of **4** obtained by polymerization of **1** by varying the feed ratio of **1** and CuCN. Dependence of (b) M_n and (c) M_w/M_n on [**1**]/[CuCN].

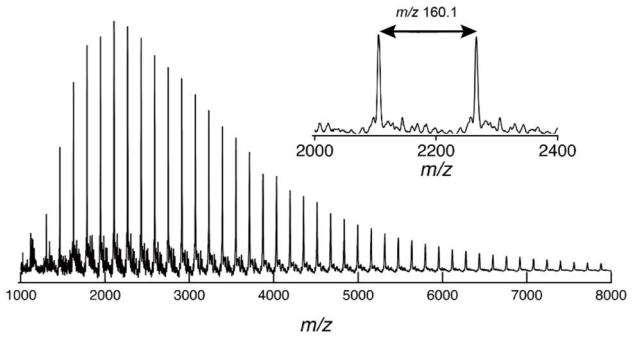

Fig. 2 MALDI-TOF-Ms spectrum of **4**.

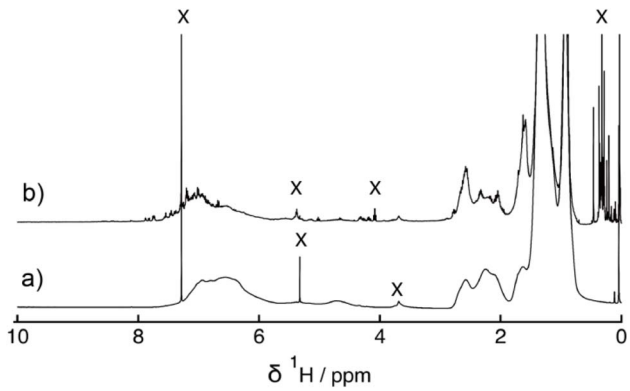

Fig. 4 ^{1}H NMR spectra of **4** (a: M_n = 7400 g mol^{-1} and b: M_n = 1200 g mol^{-1}) in $CDCl_3$ at 25 °C (X: solvent and impurity).

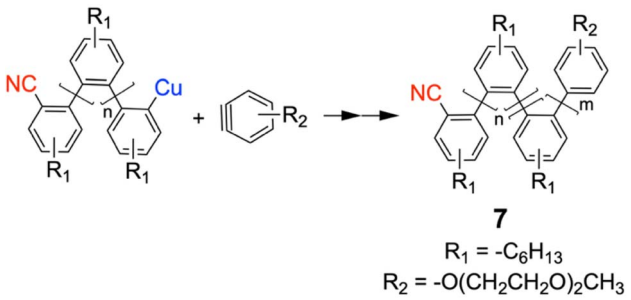

Scheme 3 Preparation of diblock P*o*P copolymer **7** from stepwise polymerization of **1** and **3**.

probably because of the steric hindrance of the two hexyl units in **2** for benzyne insertion into the terminal Cu.

o-Trimethylsilyl aryl triflate **3** with 2-(2-methoxyethoxy) ethoxy side chains was synthesized from 4-hydroxybenzaldehyde, and the hydrophilic P*o*P homopolymer **6** was obtained by the polymerization of benzyne generated from **3** under the same conditions as **4** ([**3**]/[CuCN] = 20) (Fig, S2). The P*o*P **6** is soluble in polar methanol, whereas **4** with hexyl chains is soluble in *n*-hexane, but not methanol. The M_n value and *m*/*z* peak range of **6** were slightly lower than those of **4** (Table 1). The ^{1}H NMR spectrum of **6** in $CDCl_3$ displayed aromatic proton signals at 4.4–7.3 ppm and 2-(2-methoxyethoxy)ethoxy group proton signals at 3.2–4.0 ppm (Fig. S3). The aromatic signals of **6** shifted upfield compared with those of monomer **3**. Therefore, we obtained two P*o*P homopolymers, **4** and **6**, with hydrophobic hexyl and hydrophilic 2-(2-methoxyethoxy)ethoxy side chains, respectively, by the direct polymerization of benzynes initiated by CuCN.

Next, we attempted to prepare amphiphilic diblock P*o*P copolymer **7**, which was composed of hydrophobic and hydrophilic blocks with different side chains (Scheme 3). First, benzyne generated from **1** by the fluorine anion was polymerized in the presence of CuCN at room temperature. After 1 h, a solution of **3** was added to the reaction mixture. We expected the growth of the second segment with polar side chains by the additional insertion of the second benzyne generated from **3** into the Cu terminus of the first segment with hexyl side chains. The GPC profile of **7** showed a shift toward the high-molecular-weight region by the addition of **3** and exhibited a single peak. M_n was estimated to be 10 000 g mol^{-1} with a narrow molecular weight distribution (M_n/M_w = 1.39) (Fig. 5a). The MALDI-TOF mass spectrum of **7** showed a series of peaks from *m*/*z* 2000 to 10 000 (Fig. 5b). The observed peak at *m*/*z* 3720 was consistent with the expected value for the sum of 17 mer of the hydrophobic segment, 5 mer of the hydrophilic segment, and the terminal H and CN (*m*/*z* 160.1 × 17 (the number of repeating units in the hydrophobic segment) + 194.1 × 5 (the number of repeating units in the hydrophilic segment) + 1.0 (H) + 26.0 (CN) = 3719.2) (Fig. 5c).

The ^{1}H NMR spectrum of **7** in $CDCl_3$ showed aromatic proton signals at 4.4–7.3 ppm, 2-(2-methoxyethoxy)ethoxy group proton signals at 3.2–4.0 ppm, and hexyl group proton signals at 0.6–2.7 ppm (Fig. 6a). The ratio of the signal areas of the 2-(2-methoxyethoxy)ethoxy units to those of the hexyl units in **7** was 4 : 1. The differential thermal analysis (TGA) curve of **7** revealed two steps starting at 410 and 450 °C, corresponding to the

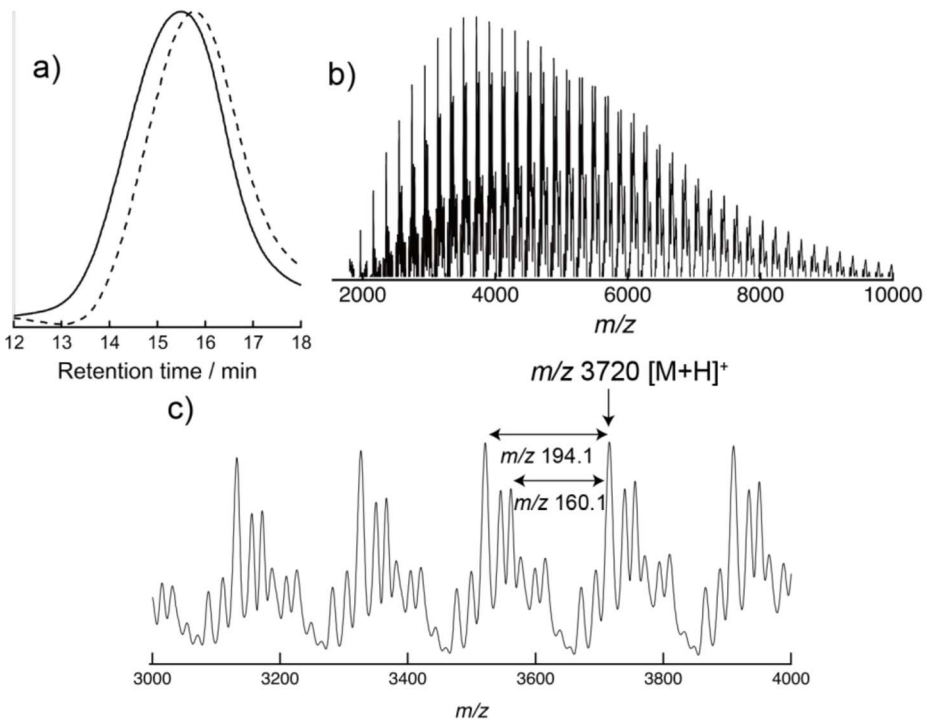

Fig. 5 (a) GPC profiles of **7** (solid line) obtained by stepwise polymerization of **1** and **3** (dotted line: polymerization of **1** with CuCN for 1 h). (b) and (c) MALDI-TOF-Ms spectrum of **7**.

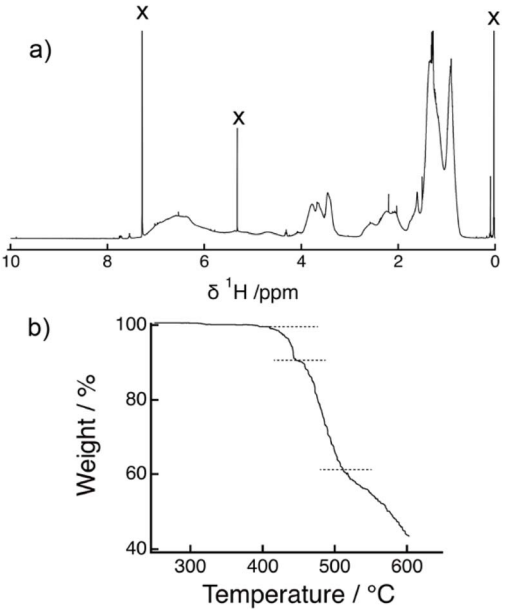

Fig. 6 (a) ^{1}H NMR spectra of **7** in $CDCl_3$ at 25 °C (X: solvent and impurity). (b) TGA profile of **7** under N_2 atmosphere.

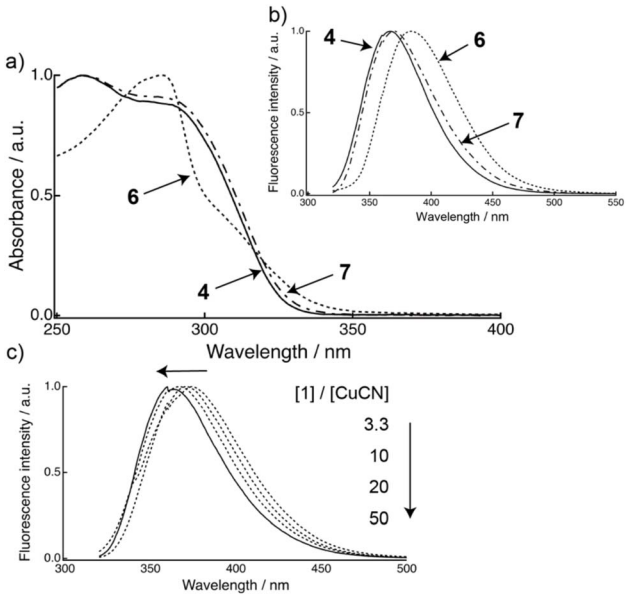

Fig. 7 (a) Absorption spectra of **4**, **6**, and **7** in dichloromethane. (b) Fluorescence spectra of **4**, **6**, and **7** in dichloromethane (ex. = 260 nm). (c) Fluorescence spectral change of **4** with increasing molecular weights (ex. = 260 nm).

thermal decomposition of the 2-(2-methoxyethoxy)ethoxy and hexyl side chains (Fig. 6b and S4). From the ratio of the two weight reductions (1 : 3) determined by TGA analysis, the average composition ratio for the two side chains in **7** was estimated to be 4 : 1, which is consistent with that determined from ^{1}H NMR spectral analysis. While the TGA curve showed no weight change below 300 °C, **7** showed two glass transition temperatures of −10 and 35 °C in differential scanning calorimetry (DSC) analysis. These results support the formation of the block copolymer by subsequent polymerization of benzyne with the hydrophilic side chain from the end of the hydrophobic P*o*P segment. However, the reverse sequence of polymerizing **3** and then adding **1** showed almost no shift of the GPC peak as compared with that of **6**, suggesting the difficulty of the subsequent growth of the second P*o*P from the terminal Cu of **6** having 2-(2-methoxyethoxy)ethoxy side chains.

The absorption and fluorescence spectra of **4**, **6**, and **7** in dichloromethane are shown in Fig. 7a. The absorption spectrum of **4** exhibited an absorption maximum at 260 nm with a shoulder peak at 296 nm. When excited at 260 nm, **4** emitted fluorescence with a peak maximum at 365 nm (Fig. 7b). As shown in Fig. 6c, a blue shift in the position of the fluorescence peak was observed as the molecular weight of **4** increased. This blue shift agrees with the result for fluorescence with increasing oligo (*ortho*-phenylene) length, as reported by Hartley *et al.*[22] The absorption/fluorescence maxima and the onset absorption value of **6** were significantly red-shifted compared to those of **4**, mainly because of the introduction of electron-donating alkoxy groups into the P*o*P backbone. The merging of the UV-Vis and fluorescence spectral features for **4** and **6** is observed in block copolymer **7**, indicating that **7** comprises both polymer segments.

A THF solution of **7** (20 μL, 1.0 mg ml^{-1}) was rapidly injected into 1.0 ml of water using a syringe to obtain a homogeneous solution, which remained dispersed for over one month without precipitation. The Tyndall effect occurs when a laser is passed through the resulting aqueous solution, indicating the presence of colloidal particles (Fig. 8a). The sample dried on a glass substrate was examined by field-emission scanning electron microscopy (FE-SEM) to verify the morphology of the colloidal particles. The FE-SEM image revealed spherical particles with diameters of 80–100 nm (Fig. 8b). To investigate the formation and stabilization process of the assemblies, a THF solution of **7** was dispersed in water, and the change in hydrodynamic diameter was monitored over time by dynamic light scattering (DLS) as THF evaporated. The particle size gradually decreased upon the removal of THF and reached a stable equilibrium state after approximately 2 hours. The resulting average diameter was 131 ± 39 nm (Fig. S5), which is in good agreement with the spherical particles (80–100 nm) observed in FE-SEM. The fluorescence spectrum of **7** dispersed in

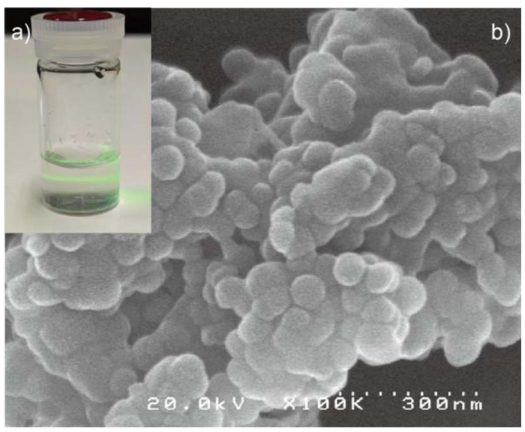

Fig. 8 (a) Laser light scattering of aqueous dispersion of **7**. (b) FE-SEM image of spherical organizations made of **7**.

water was almost the same as that in dichloromethane, suggesting the isolation of the Po**P** backbone in the spherical assemblies (Fig. S6). Amphiphilic block copolymer **7** can be organized into spherical assemblies by assembling its hydrophobic segments without stacking of the Po**P** backbones.

Conclusions

In conclusion, we have demonstrated the stepwise direct polymerization of two benzynes to construct diblock poly(*ortho*-phenylene) copolymers. The attachment of two hexyl groups at the 3 and 4 positions of *o*-trimethylsilyl aryl triflates inhibited the smooth growth of poly(*ortho*-phenylene) due to steric hindrance, resulting in a lower molecular weight than the expected value calculated from the feed ratio of *o*-trimethylsilyl aryl triflate and CuCN. In contrast, the polymerization of other benzynes generated from **1** and **3** with single hexyl or 2-(2-methoxyethoxy)ethoxy side chains proceeded smoothly at room temperature to give poly(-*ortho*-phenylene)s with narrow molecular weight distributions. Diblock poly(*ortho*-phenylene) copolymers were prepared by polymerizing the second benzyne at the end of the poly(*ortho*-phenylene) derived from the first benzyne. The formation of spherical assemblies of amphiphilic diblock poly(*ortho*-phenylene) copolymers, consisting of a linear arrangement of two blocks with hydrophobic and hydrophilic side chains in water, was also investigated. This synthetic approach may open new possibilities for various applications by designing well-defined poly(*ortho*-phenylene)-based block copolymers. However, the current study has certain limitations. The chain growth and achievable molecular weights are restricted by severe steric hindrance when monomers with bulky side chains are employed. Additionally, the successful formation of block copolymers is currently highly dependent on the monomer addition sequence. To address these challenges, future studies will focus on optimizing the catalytic conditions to overcome these synthetic limitations and expand the monomer scope. Furthermore, detailed structural characterizations using multi-angle light scattering (MALS) are currently underway to further explore their fundamental solution properties.

Author contributions

Masahiro Sonobe: conceptualization, investigation, formal analysis, data curation, visualization. Yu Kitazawa: investigation, validation. Masanobu Uchiyama: conceptualization, methodology. Mutsumi Kimura: conceptualization, supervision, funding acquisition, project administration, writing – review & editing.

Conflicts of interest

The authors declare no conflict of interest.

Data availability

The data supporting this article have been included as part of the supplementary information (SI). Supplementary information is available. See DOI: https://doi.org/10.1039/d6ra01918h.

Acknowledgements

This work has been partially supported by JSPS KAKENHI (No. 15H02172 for K. M.) and the Asahi Glass Foundation.

References

1 B. A. Hammer and K. Müllen, *Chem. Rev.*, 2016, **116**, 2103–2140.
2 J. He, S. M. Mathew, S. D. Cornett, S. C. Grundy and C. S. Hartley, *Org. Biomol. Chem.*, 2012, **10**, 3398–3405.
3 E. Ohta, H. Sato, S. Ando, A. Kosaka, T. Fukushima, D. Hashizume, M. Yamasaki, K. Hasegawa, A. Muraoka, H. Ushiyama, K. Yamashita and T. Aida, *Nat. Chem.*, 2011, **3**, 68–73.
4 S. Ando, E. Ohta, A. Kosaka, D. Hashizume, H. Koshino, T. Fukushima and T. Aida, *J. Am. Chem. Soc.*, 2012, **134**, 11084–11087.
5 T. Kajitani, Y. Suna, A. Kosaka, T. Osawa, S. Fujikawa, M. Takata, T. Fukushima and T. Aida, *J. Am. Chem. Soc.*, 2013, **135**, 14564–14567.
6 S. Mathew, L. A. Crandall, C. J. Ziegler and C. S. Hartley, *J. Am. Chem. Soc.*, 2014, **136**, 16666–16675.
7 C. S. Hartley, *Acc. Chem. Res.*, 2016, **49**, 646–654.
8 A. J. Blake, P. A. Cooke, K. J. Doyle, S. Gair and N. S. Simpkins, *Tetrahedron Lett.*, 1998, **39**, 9093–9096.
9 S. M. Mathew and C. S. Hartley, *Macromolecules*, 2011, **44**, 8425–8432.
10 H. Arslan, K. L. Walker and W. R. Dichtel, *Org. Lett.*, 2014, **16**, 5926–5929.
11 E. Ihara, A. Kurokawa, T. Koda, T. Muraki, T. Itoh and K. Inoue, *Macromolecules*, 2005, 2167–2172.
12 S. Ito, K. Takahashi and K. Nozaki, *J. Am. Chem. Soc.*, 2014, **136**, 7547–7550.
13 Y. Mizukoshi, K. Mikami and M. Uchiyama, *J. Am. Chem. Soc.*, 2015, **137**, 74–77.
14 H.-C. Kim, S.-M. Park and W. D. Hinsberg, *Chem. Rev.*, 2010, **110**, 146–177.
15 Y. Himeshima, T. Sonoda and H. Kobayashi, *Chem. Lett.*, 1983, **12**, 1211–1214.
16 D. Peña, D. Pérez, E. Guitián and L. Castedo, *J. Am. Chem. Soc.*, 1999, **121**, 5827–5828.
17 D. Peña, D. Pérez, E. Guitián and L. Castedo, *J. Org. Chem.*, 2000, **65**, 6944–6950.
18 H. Yoshida, J. Ikadai, M. Shudo, J. Ohshita and A. Kunai, *J. Am. Chem. Soc.*, 2003, **125**, 6638–6639.
19 K. Tamao, K. Sumitani and M. Kumada, *J. Am. Chem. Soc.*, 1972, **94**, 4374–4376.
20 R. J. P. Corriu and J. P. Masse, *J. Chem. Soc. Chem. Commun.*, 1972, 144a.
21 S. Mathew, L. A. Crandall, C. J. Ziegler and C. S. Hartley, *J. Am. Chem. Soc.*, 2014, **136**, 16666–16675.
22 J. He, J. L. Crase, S. H. Wadumethrige, K. Thakur, L. Dai, S. Zou, R. Rathore and C. S. Hartley, *J. Am. Chem. Soc.*, 2010, **132**, 13848–13857.